AD-A043 496 CASE WESTERN RESERVE UNIV CLEVELAND OHIO ULTRASONICS --ETC F/G 9/1
GENERATION OF ULTRASOUND AT METAL ELECTROLYTE INTERFACES.(U)
AUG 77 F BORSAY, E YEAGER N00014-75-C-0557

UNCLASSIFIED TR-44 NL

| OF |
AD
A043496

END
DATE
FILMED
9 -77
DDC

(6)

# ULTRASONICS RESEARCH LABORATORY

DEPARTMENT OF CHEMISTRY
JOHN SCHOFF MILLIS SCIENCE CENTER

## CASE WESTERN RESERVE UNIVERSITY

Cleveland, Ohio

TECHNICAL REPORT NO. 44

# GENERATION OF ULTRASOUND AT METAL ELECTROLYTE INTERFACES

by

Frank Borsay and Ernest Yeager

4 August 1977

OFFICE OF NAVAL RESEARCH

Contract N00014-75-C-0557

Project NR 384-305

OFFICE OF NAVAL RESEARCH

Contract N00014-75-C-0557
Project NR 384-305

TECHNICAL REPORT NO. 44

# GENERATION OF ULTRASOUND AT METAL ELECTROLYTE INTERFACES

by

Frank Borsay and Ernest Yeager

Ultrasonics Research Laboratory
Department of Chemistry
Case Western Reserve University
Cleveland, Ohio 44106

4 August 1977

Unclassified

SECURITY CLASSIFICATION OF THIS PAGE (When Data Entered)

| REPORT DOCUMENTATION PAGE | READ INSTRUCTIONS BEFORE COMPLETING FORM |
|---|---|
| 1. REPORT NUMBER: (14) TR-44 / 2. GOVT ACCESSION NO. | 3. RECIPIENT'S CATALOG NUMBER |
| 4. TITLE (and Subtitle): GENERATION OF ULTRASOUND AT METAL ELECTROLYTE INTERFACES | 5. TYPE OF REPORT & PERIOD COVERED: Technical Report, |
| | 6. PERFORMING ORG. REPORT NUMBER |
| 7. AUTHOR(s): (10) Frank Borsay and Ernest Yeager | 8. CONTRACT OR GRANT NUMBER(s): (15) N00014-75-C-0557 |
| 9. PERFORMING ORGANIZATION NAME AND ADDRESS: Ultrasonics Laboratory, Case Western Reserve University, Department of Chemistry, Cleveland, Ohio 44106, U.S.A. | 10. PROGRAM ELEMENT, PROJECT, TASK AREA & WORK UNIT NUMBERS: NR 384-305 |
| 11. CONTROLLING OFFICE NAME AND ADDRESS: Office of Naval Research, Arlington, Va. 22217, Physics Section, Code 421 | 12. REPORT DATE: (11) 4 August 1977 |
| | 13. NUMBER OF PAGES: ~~27~~ (12) 22p. |
| 14. MONITORING AGENCY NAME & ADDRESS(if different from Controlling Office) | 15. SECURITY CLASS. (of this report): Unclassified |
| | 15a. DECLASSIFICATION/DOWNGRADING SCHEDULE |

16. DISTRIBUTION STATEMENT (of this Report)

Approved for public release; distribution unlimited

17. DISTRIBUTION STATEMENT (of the abstract entered in Block 20, if different from Report)

18. SUPPLEMENTARY NOTES

19. KEY WORDS (Continue on reverse side if necessary and identify by block number)

ultrasound, sound generation, metal-electrolyte interface, ionic double layer, electrochemistry

20. ABSTRACT (Continue on reverse side if necessary and identify by block number)

When a radiofrequency potential is applied to an electrode such as gold in an electrolyte, ultrasound is generated at the interface. This effect is attributed to changes in the volume of the solution adjacent to the metal and can be used to study the structure of the interface. Preliminary measurements are reported as a function of the d.c. electrode potential. The effect is particularly sensitive to adsorbed species such as organics. Various means for enhancing the effect are discussed.

DD FORM 1 JAN 73 1473 EDITION OF 1 NOV 65 IS OBSOLETE

S/N 0102-LF-014-6601

Unclassified

SECURITY CLASSIFICATION OF THIS PAGE (When Data Entered)

TABLE OF CONTENTS

LIST OF FIGURES

Technical Report No. 44

# GENERATION OF ULTRASOUND AT METAL ELECTROLYTE INTERFACES

by

Frank Borsay and Ernest Yeager

## I. INTRODUCTION

When an a.c. potential is applied to an electrochemical interface, periodic volume changes are produced at the interface. This in turn should give rise to the generation of sound waves of the same frequency in the solution phase. This report describes the first detection of these sound waves using a gold electrode in an acid electrolyte. This effect offers a means for examining the potential dependence of the structure of the compact double layer at metal-electrolyte interfaces.

## II. MECHANISTIC CONSIDERATIONS

The solution side of a metal-electrolyte interface consists of two layers, a compact layer corresponding to the distance of closest approach of the ions to the metal surface and a diffuse ion layer (Gouy-Chapman) extending out into the electrolyte phase (see Fig. 1). [For reviews, see refs. 1,2.] In the absence of strong (specific) ionic adsorption, the plane of closest approach of the ions (the Helmholtz plane) in aqueous solutions is normally assumed to be separated from the metal surface by two water molecules, one in direct contact with the metal surface and the second in the inner (primary) hydration sheath of the ions making up this plane. Except at or near the potential of zero charge (pzc) (i.e. $\phi_M - \phi_H = 0$), the

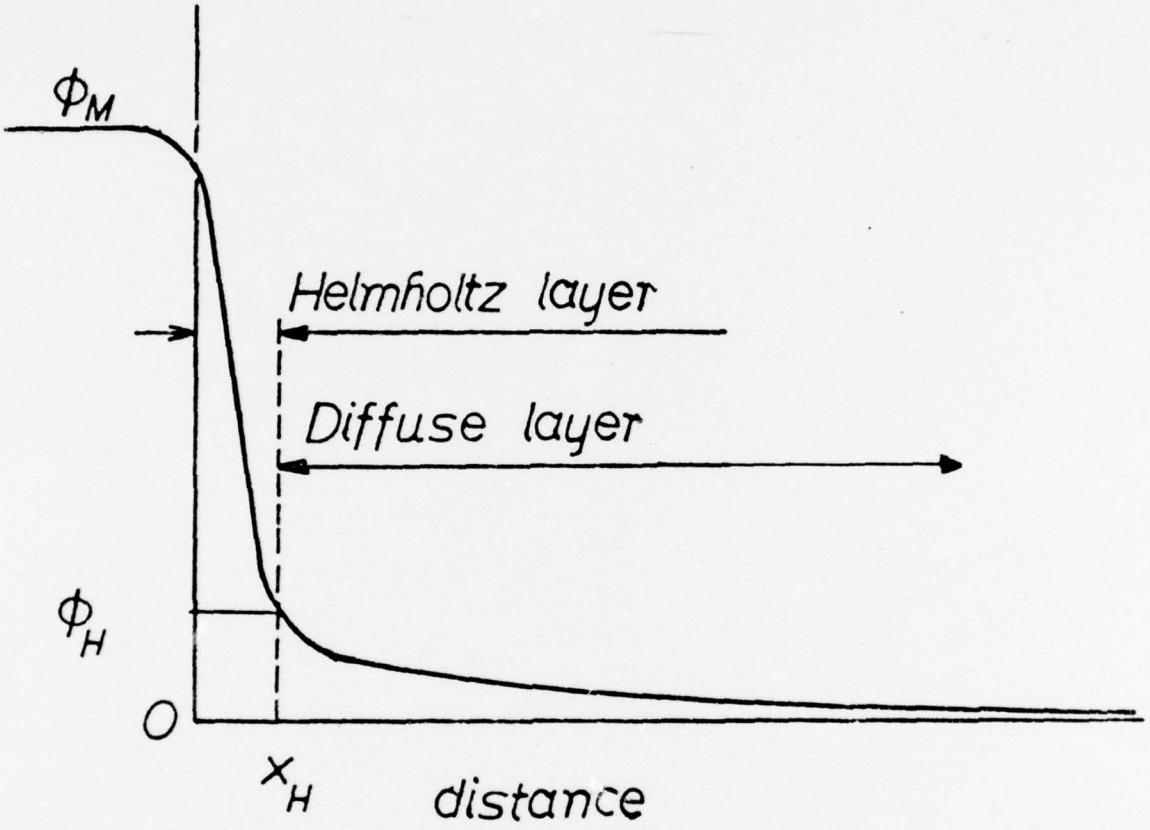


Figure 1. Potential distribution across a metal-electrolyte interface.

Helmholtz plane consists of predominantly only cations or anions, depending on the sign of the potential.

At ordinary electrolyte concentrations ($>10^{-2}$M) most of the potential drop between the bulk metal and bulk electrolyte is between the metal and Helmholtz plane. Consequently the water in the compact layer is subject to a large potential gradient except at or near the pzc (up to $10^{8}$V/cm). Such gradients can produce large changes in the structure of the water layer, including re-orientation of the water dipoles from predominantly towards to away from the surface. This should result in substantial volume changes with changes in the potential applied across the interface.

Acoustical methods appear an attractive approach for examining these changes in the structure of the compact layer with applied potential. Even a volume change of only 1% should result in a displacement of $\sim 3\times10^{-10}$ cm and, at a modulation frequency of e.g. 500 kHz, sound waves of $10^{-8}$W/cm$^2$, which is easily detected.

Changes in the ion distribution in the ionic double layer will also contribute to the acoustic effect. This contribution would not occur if the ions of the double layer behaved ideally. Any increase or decrease in volume within the layer due to a change of ion concentrations would be offset by a volume change of opposite sign in the bulk solution adjoining the electrode surface within a distance small compared to the acoustic wavelength for frequencies below $10^{8}$Hz. The ion concentration in the diffuse layer, however, can reach values high compared to the bulk concentrations when $\phi_M$ (see Fig. 1) becomes sub-

stantial ($|\phi_M|>0.1V$). Ion pair and triplet formation results in a loss of some water in the outer and inner ionic hydration sheaths and, therefore, increments in the ionic partial molal volumes and net volume of the solution adjacent to the electrode surface. The entrance of ions into the Helmholtz plane results also in changes in their partial molal volumes because of changes in the outer (secondary) hydration sheaths. Further, the specific adsorption of ions into direct contact with the metal surface will occur with most electrolytes at sufficiently negative or positive potential and this should produce large volume increments due to the displacement of water molecules from the interface as well as ion hydration sheaths. The extent to which these various sources of volume changes contribute to the observed acoustic effect depends on the particular electrolyte, metal electrode and the potential relative to the pzc. With a strong acid electrolyte such as $HClO_4$, which only weakly adsorbs on noble metals and has only minor concentration dependence of the ionic partial molal volumes, the volume changes associated with the compact layer are expected to be predominant.

Quantitative treatments of the potential dependence of the volume of the compact layer can be carried out with various models of this layer; e.g. the multiple-state models of the compact layer water proposed by Damaskin and Frumkin (3.4), Parsons (5), Bockris and Habib (6). This together with a treatment of other contributions to the volume changes will be the subject of a future publication. This effect should prove useful in testing these models.

The relation of this effect to the theoretical models for the interface water structure can be illustrated as follows, using the Damaskin modification (4) of the Damaskin - Frumkin multistate model (3) of the compact layer structure. According to this treatment, the water at the interface in the absence of specific ionic adsorption exists in the form of small clusters with chemisorption of individual water molecules occurring at more positive electrode potentials. Using Boltzmann statistics, the surface concentration of the clusters can be calculated, assuming that the clusters consist of a fixed number of water molecules (n) and have their dipole moments oriented toward ($N\uparrow_c$) or away ($N\downarrow_c$) from the metal surface. If $N_T$ is the total number of entities on the surface, then

$$N_T = N\uparrow_c + N\downarrow_c + N_{ad} \tag{1}$$

and the volume is

$$V_T = (N\uparrow_c)(V\uparrow_c) + (N\downarrow_c)(V\downarrow_c) + (N_{ad})(V_{ad}) \tag{2}$$

where the V's are the corresponding effective volumes. The number of species per unit area can be evaluated with

$$N\uparrow_c/N_T = (1/f_o) \exp(\mu_c X/kT) \tag{3}$$

$$N\downarrow_c/N_T = (1/f_o) \exp(-\mu_c X/kT) \tag{4}$$

$$N_{ad}/N_T = (1/f_o) \exp[(-U + \mu_{ad} X)/kT] \tag{5}$$

with the function $f_o$

$$f_o = \exp(\mu_c X/kT) + \exp(-\mu_c X/kT) + \exp[(-U \pm \mu_{ad} X)/kT] \tag{6}$$

and $N_{ad}$ corresponds to the chemisorbed water molecules with the dipole moment $\mu_{ad}$ and specific adsorption energy U at zero field X. A subtended area is assigned to each of these three species and a conservation of surface area condition imposed. The potential drop across the

compact layer $\Delta\phi = \phi_M - \phi_H$ (see Fig. 1) is then assumed to be

$$\Delta\phi = \Delta\psi + \Delta\chi \tag{7}$$

where the outer potential contribution $\Delta\psi$ is given by

$$\Delta\psi = \frac{4\pi x_2}{\epsilon} q \tag{8}$$

and the surface potential contribution is

$$\Delta\chi = \frac{-4\pi}{\epsilon} \Sigma N_i \mu_i \tag{9}$$

and i corresponds to the two orientations of the water clusters and the chemisorbed water; q is the electrode charge. Following Damaskin's approach discreteness-of-charge effects can be introduced through a coefficient $\lambda$ which is intended to take into account the action of the field of all other dipoles on the particular dipole under consideration. Thus

$$\chi = \frac{4\pi q}{\epsilon} + \lambda \frac{\Delta\chi}{x_2} = \frac{\Delta\phi}{x_2} \tag{10}$$

Then V can be obtained as a function of $\Delta\phi$ and hence applied potential since for concentrated electrodes $\Delta\phi = \phi_M$ (see Fig. 1) to a good approximation. The acoustic amplitude can then be obtained from dV/dE where E is the applied potential relative to a reference electrode.

The number of constants to be introduced is a problem; i.e., the volumes, dipole moments, adsorption energies and subtended surface areas of the various species. These can be estimated on the basis of models for the various species but not with great accuracy. The approach of Bockris and Habib (6,7) may prove of some help since it evaluates the partition functions for the various structures.

When ionic contributions must be considered, similar equations can be set up in terms of the volume change attending specific adsorption and also ion pair and triplet formation in the ionic double layer. The electromodulation of the surface concentration of adsorbed ions can be calculated under equilibrium conditions from the adsorptions isotherms, evaluated for example optically (11). At frequencies in the ultrasonic range, however, kinetic and diffusional factors will also need to be considered.

The development of the detailed treatment of this effect is in progress along these lines.

## III. APPARATUS AND TECHNIQUES

To differentiate this electroacoustic effect from electromagnetic cross talk, the measurements have been carried out with pulse-modulation techniques using the differences in the propagation velocities of acoustic and electromagnetic waves, with the arrangement shown in Fig. 2. An acoustic frequency of 540 kHz was used for this study. At frequencies below those at which interfacial relaxation occur ($<10^6$ Hz in the absence of specific adsorption), the volume change with potential is independent of frequency. Therefore under ideal circumstances, the acoustic intensity is related to the displacement amplitude $a_o$ and hence the volume changes by the expression $I = 1/2\ \omega^2 a_o^2$ where $\omega$ is the angular frequency. Consequently the higher the frequency, the greater is the intensity. The frequency range $10^5$ to $10^6$ Hz, however, is best suited to quantitative acoustic measurements. At higher frequencies, the short wavelength requires much thinner diaphragms and leads to more problems with alignment and acoustic losses. At lower frequencies, large diaphragms and tanks are required to reduce diffraction and cope with band width-delay time restrictions with tuned amplifiers.

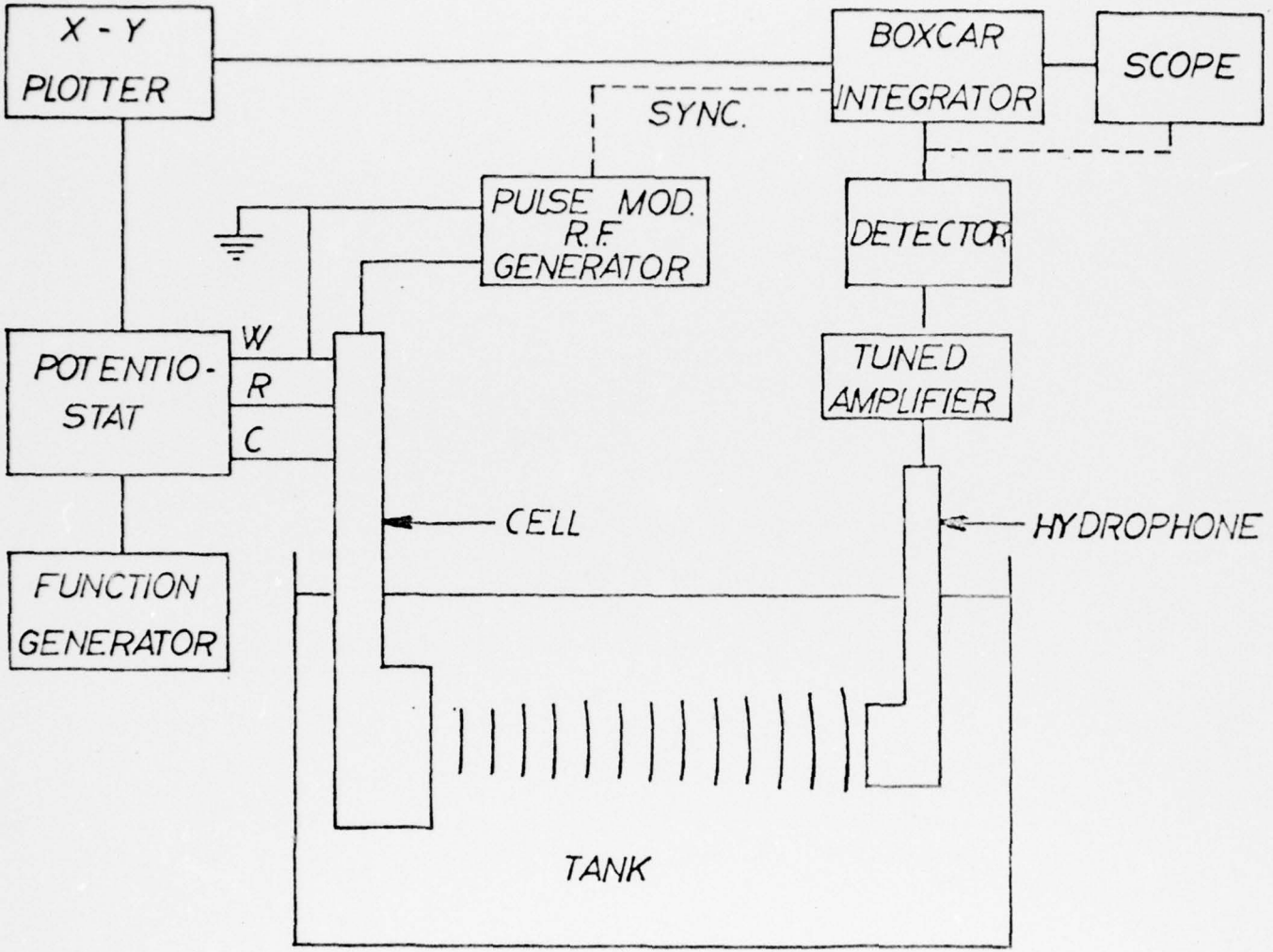


Figure 2. Apparatus for acousto-electrochemical measurements. Potentiostat: PAR Model 176. Function generator: PAR Model 175. Pulse modulated r.f. generator: Arenberg Model PG-650-C. Boxcar integrator: PAR Model 160.

The acousto-electrochemical cell and the detection transducer were mounted within a water filled tank affording acoustic delay times up to 1 ms. The detection transducer was a 4.0 -cm circular barium titanate plate with a ∿540 kHz fundamental. The source of modulation potential and detection electronics are shown in the block diagram (Fig. 2).

The acoustic-electrochemical cell arrangement (Fig. 3) provided a means for isolating the metal-electrolyte interface from the water of the tank. This permitted the maintenance of far higher purity control in the electrolyte than would be possible if the acoustic waves were detected in the electrolyte. The cell body was constructed of Teflon with an outer brass case to provide shielding and rigidity. The pulse-modulated radio-frequency potential (540 kHz) was applied between one side of a gold diaphragm and a parallel gold screen (200 mesh). The gold diaphragm was sufficiently thin (0,013 cm) that sound generated at the diaphragm and mesh electrodes was transmitted into the water of the tank with little attenuation. The diameter of the sections of the gold diaphragm and mesh exposed to the electrolyte was 2.54 cm. This is large compared to the wavelength in the solution and hence the energy in the diffraction lobes is rather small.

The dc potential of the gold diaphragm was controlled relative to a saturated calomel reference electrode (SCE) by means of a potentiostat using a gold counter electrode of 10-$cm^2$ area located behind the grid electrode (see Fig. 3). The cell also included a gold pre-electrolysis anode and cathode for removing impurities by pre-electrolysis. In the preliminary measurements reported herein, the dc potential of the mesh electrode was not controlled.

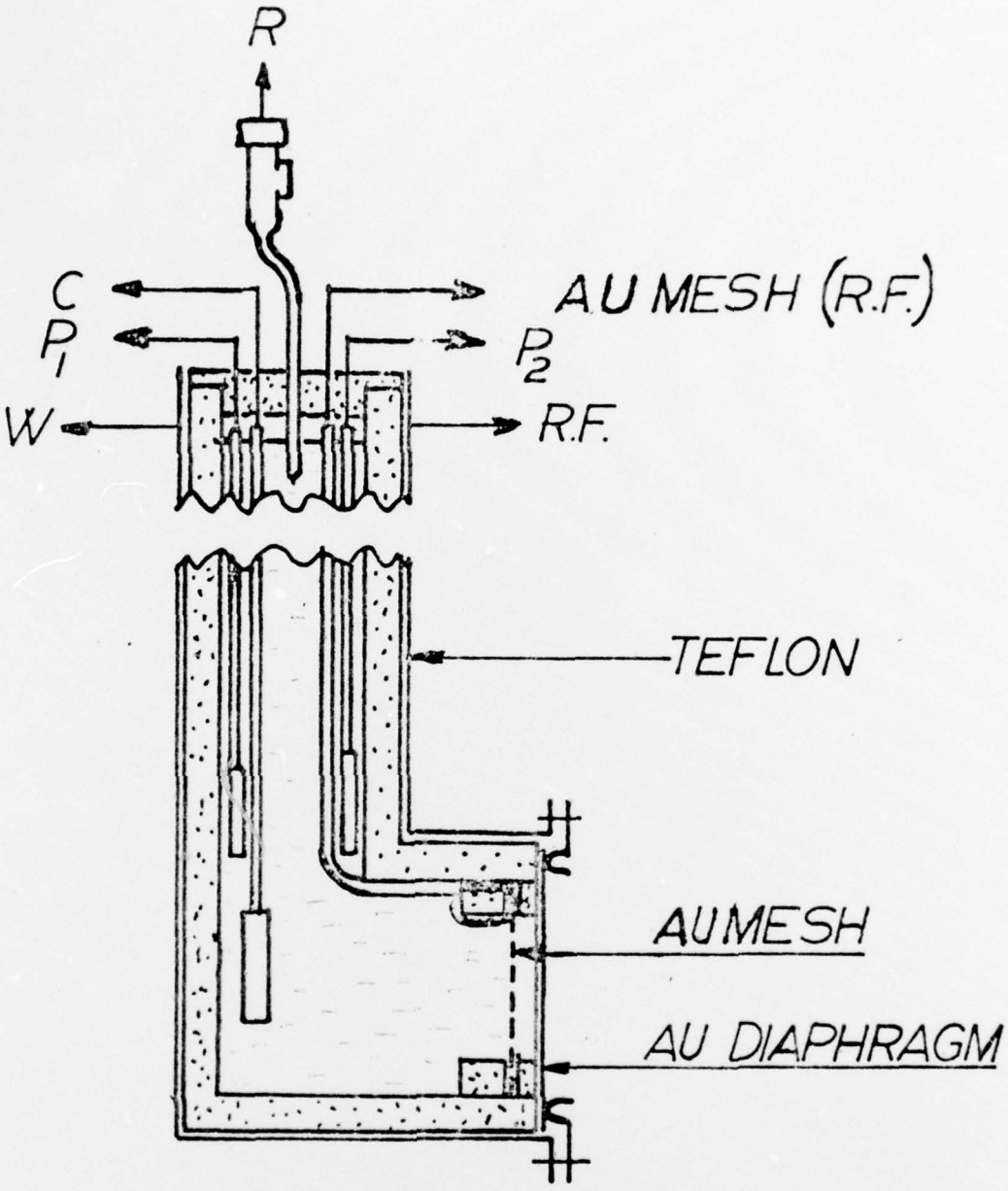


Figure 3. Acousto-electrochemical cell R.- saturated calomel reference electrode. $P_1$, $P_2$ - pre-electrolysis electrodes (Au). C - counter electrode for controlling dc potential of Au diaphragm electrode.

The acoustic response has been recorded while linearly sweeping the dc voltage of the gold diaphragm electrode in a positive and then negative direction. The modulation voltage applied between the two parallel electrodes appears principally across the electrolyte resistance with only a small fraction at the two interfaces. The interface impedances are mostly capacitive with the value dependent on the dc potential. At potentials in the range -0.2 to 0.7V(SCE)the capacitance for bright gold in 2M $HClO_4$ is typically 30 to 40$\mu F/cm^2$ with only minor dependence on dc potential. For this electrolyte, the resistance between the diaphragm and mesh electrodes is calculated to be 0.14 ohms at audio frequencies using a Wayne-Kerr bridge (model B221). Assuming the area in contact with the electrolyte to be approximately the same for the diaphragm and mesh electrodes, the estimated fraction of the total applied modulation voltage across each interface is $2.6 \times 10^{-3}$.

The volume changes at the mesh electrode are 180° out of phase with those at the diaphragm at the same dc potential. To obtain proper phase relations between sound generated at the two electrodes, the spacing has been adjusted to one half wavelength (0.139 cm at 540 kHz). The cell has not been optimized, however, for the standing waves reflected of the Teflon end.

## IV. RESULTS

The relative acoustic response is shown in Fig. 4. These results must be considered rather preliminary since the electrolyte may have contained sufficient impurities including $Cl^-$ ions to disturb the interface properties. Extreme purification procedures are necessary to assure adequate purity for such experiments and will be used in later work.

The voltammetry curves, however, have been examined under similar conditions in this cell and found to be essentially the same as published earlier (7, 8) from our laboratory in purified electrolytes. The acoustic signal in Fig. 4 includes a contribution from the gold mesh electrode, which, while unknown, was constant. This unknown component makes it impossible to establish whether the acoustic signal passes through zero with a 180° - phase change at any potential in the range shown in Fig. 4. In future work the potential of both of the parallel r-f electrodes will be maintained the same, so as to insure constructive interference with a half wavelength spacing and hence to know the zero acoustic signal condition for both electrodes.

The behavior indicated in the "voltacoustogram" in Fig. 4 seems quite reasonable. The voltage region with the large hysteresis at potentials positive to 0.8V vs SCE corresponds to the very irreversible formation and reduction of an anodic oxide layer at a monomolecular level. The formation of this film results in a pronounced change in the intrinsic properties of the interface as well as a substantial change in the electrode capacitance and hence fraction of the modulation voltage across the interface. The region negative to 0.7V is free of hysteresis as is to be expected for gold in the "anion region" where the potential is positive to the pzc but only a small amount of specific adsorption of $ClO_4^-$ anions occurs. [For gold in 2M $HClO_4$, the pzc is estimated to be $\sim$-0.3V vs SCE from literature data (9, 10).] At the sweep rate of 50mV/s used in this experiment, the residual $Cl^-$ (estimated at $\sim 10^{-6}$M in the $HClO_4$) should have relatively little effect even though this ion rather strongly adsorbs on gold.

The addition of organics such as benzene (Fig. 5) to the electrolyte has a major effect on the magnitude and potential dependence of the effect. This is not surprising since such species adsorb strongly on the electrode

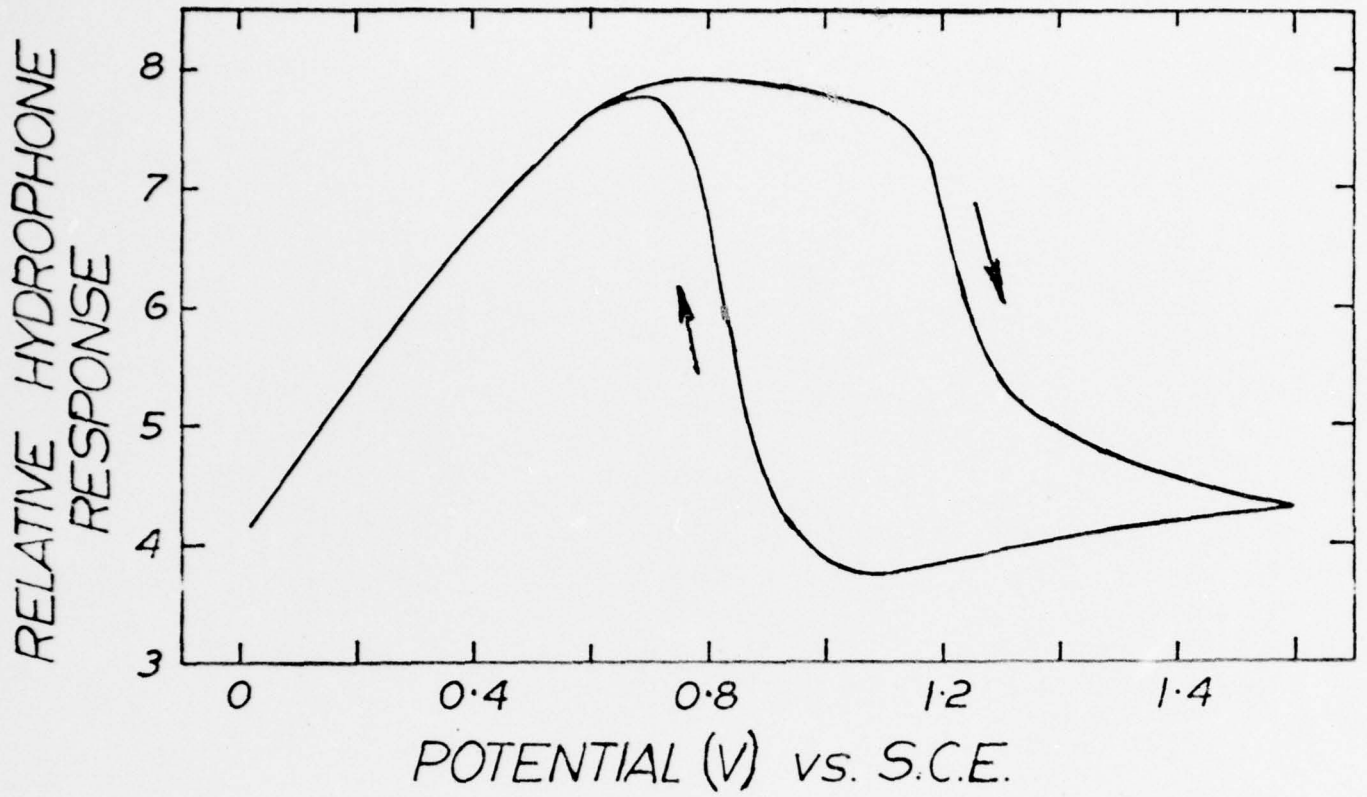


Figure 4. Relative acoustic response for gold in 2M $HClO_4$. Total modulation voltage amplitude: 4.0V; modulation frequency: 540 kHz. Sweep voltage rate: 50 mV/s; sweep directions indicated by arrows. Temp.: ~25°C. Solution helium saturated and pre-electrolyzed for 12 hr to reduce impurity content.

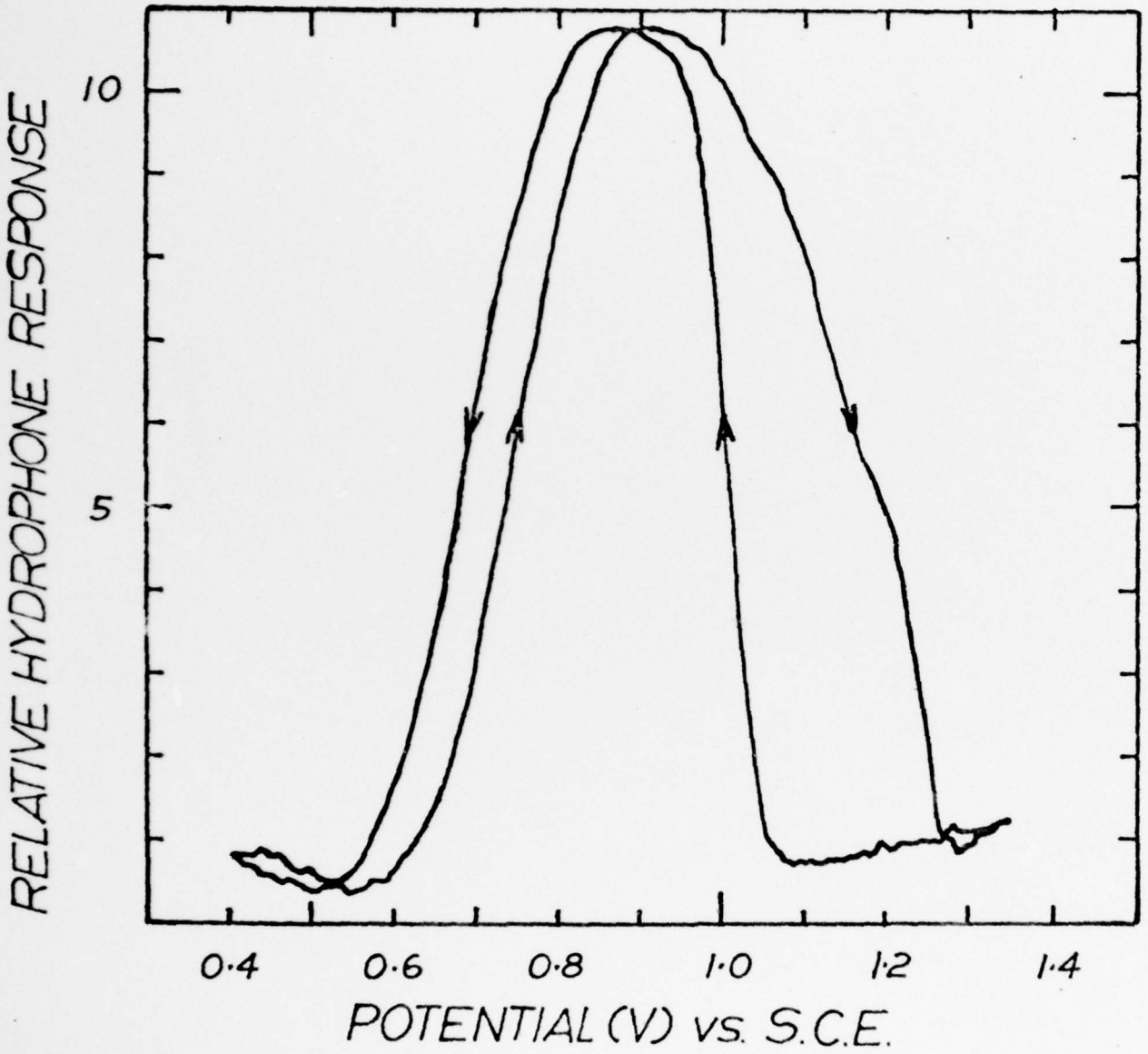


Figure 5. Relative acoustic response for gold in 2M $HClO_4$ + 7.873 x $10^{-4}$M Benzene. Total modulation voltage amplitude: 4.0V; modulation frequency: 540 kHz; Bias voltage sweep rate: 10 mV/sec; Temperature: ~25°C.

at various potentials and can also undergo Faradaic processes yielding various oxidation and reduction products. The adsorbed species change the potential distribution across the interface. The structural changes produced by the potential modulation become considerably more complex since they involve the adsorbed species as well as water molecules. At low modulation frequencies ($<10^4$ Hz), the ac potential modulation will in turn modulate the surface concentration of the adsorbed species and hence with the volume change will produce an additional volume modulation component associated with the change of the partial molal volume of the species with adsorption-desorption. At frequencies above $10^5$ Hz, however, the adsorption-desorption process is likely to be too slow to follow the a.c. modulation because of diffusion restrictions at the low concentrations of these species. The acoustic response provides a sensitive readout for recognizing adsorption at metal-electrolyte interfaces and may prove useful for this purpose in research on such interfaces

On the basis of a radiation pressure calibration of the hydrophone using a second acoustic source at 540 kHz, the rms acoustic velocity corresponding to 0.8 units for the $2\underline{M}$ $HClO_4$ curve in Fig. 4 is estimated to be $10^{-9}$ W/cm$^2$ at a distance of 135 cm from the gold diaphragm source. This value seems reasonable in terms of a few tenths of a percent change in the volume of the double layer for a $\Delta\phi_H$ -modulation amplitude of $\sim$15 mV for each electrode.

This acousto-electrochemical effect is expected to prove a useful readout of uncompensated volume changes at electrochemical interfaces and particularly a test for various models of the compact double layer. Quantification of the measurements requires careful design of the cell; this is progress.

This effect is too small to be a practical source for sound generation. It is possible, however, to enhance the effect by stacking a number of very thin electrodes with very small electrolyte gaps (e.g. $10^{-2}$ cm or less). The metal electrodes can be bipolar, i.e., expose different metal surfaces on opposite sides with the metals chosen to give the proper phase relation. With such an arrangement, most of the applied a.c. potential will be across the interfaces. Under such circumstances much greater volume changes and hence acoustic amplitudes can be obtained from each interface through the use of high surface area forms of the metals such as gold and platinum metal blacks. At a given frequency, enhancement of the effect by 60dB should be possible. Such transducers may prove interesting for laboratory generation of ultrasound when a broad band transducer is required.

Acknowledgments: The authors acknowledge useful discussions with Dr. W. E. O'Grady and Dr. A. Soffer (Abrams Foundation Fellow at Case Western Reserve University).

References

1. See e.g., C. A. Barlow, Jr. and J. R. MacDonald, "Theory of Discreteness of Charge Effects in the Electrolyte Compact Double Layer", in Advances in Electrochemistry and Electrochemical Engineering, P. Delahay and C. Tobias, eds., J. Wiley and Sons, New York, 1967.

2. C. A. Barlow, Jr., "The Electrical Double Layer", in Physical Chemistry, An Advanced Treatise, Vol. IXA, Chapter 2, H. Eyring, D. Henderson and W. Jost, eds., Academic Press, New York City, 1970.

3. B. B. Damaskin and A. N. Frumkin, Electrochim. Acta 19, 173 (1974).

4. B. B. Damaskin, J. Electroanal. Chem. 75, 359 (1977).

5. R. Parsons, ibid. 59, 229 (1975).

6. J. O'M. Bockris and M. A. Habib ibid. 65, 473 (1975); Electrochim. Acta, in press.

7. R. Adzic, J. Horkans, B. D. Cahan and E. Yeager, J. Electrochem. Soc. 120, 1219 (1973).

8. J. Horkans, B. D. Cahan and E. Yeager, Surface Sci. 46, 1 (1974).

9. D. D. Bode, T. N. Anderson and H. Eyring, J. Phys. Chem. 71, 792 (1967).

10. M. Green and H. Dahms, J. Electrochem. Soc. 110, 466 (1963).

11. R. Adzic, E. Yeager and B. D. Cahan, J. Electroanal. Chem., in press.

TECHNICAL REPORT DISTRIBUTION LIST

CASE WESTERN RESERVE UNIVERSITY

Contract N00014-75-C-0557 Project NR 384-305

| | |
|---|---|
| Director<br>Defense Advanced Research Projects Agency<br>Attn: Technical Library<br>1400 Wilson Blvd.<br>Arlington, Virginia 22209 | 3 copies |
| Office of Naval Research<br>Physics Program Office (Code 421)<br>800 North Quincy Street<br>Arlington, Virginia 22217 | 3 copies |
| Office of Naval Research<br>Assistant Chief for Technology (Code 200)<br>800 North Quincy Street<br>Arlington, Virginia 22217 | 1 copy |
| Naval Research Laboratory<br>Department of the Navy<br>Attn: Technical Library<br>Washington, D. C. 20375 | 3 copies |
| Office of the Director of Defense<br>Research and Engineering<br>Information Office Library Branch<br>The Pentagon<br>Washington, D. C. 20301 | 3 copies |
| U. S. Army Research Office<br>Box CM, Duke Station<br>Durham, North Carolina 27706 | 2 copies |
| Defense Documentation Center<br>Cameron Station (TC)<br>Alexandria, Virginia 22314 | 12 copies |
| Director, National Bureau of Standards<br>Attn: Technical Library<br>Washington, D. C. 20234 | 1 copy |
| Commanding Officer<br>Office of Naval Research Branch Office<br>536 South Clark Street<br>Chicago, Illinois 60605 | 3 copies |

San Francisco Area Office — 3 copies
Office of Naval Research
760 Market Street, Room 447
San Francisco, California 94102

Office of Naval Research — 6 copies
Code 102 1P (ONR/L)
800 North Quincy Street
Arlington, Virginia 22217

Air Force Office of Scientific Research — 1 copy
Department of the Air Force
Washington, D. C. 22209

Commanding Officer — 3 copies
Office of Naval Research Branch Office
1030 East Green Street
Pasadena, California 91101

Commanding Officer — 3 copies
Office of Naval Research Branch Office
495 Summer Street
Boston, Massachusetts 02210

Director — 1 copy
U. S. Army Engineering Research
and Development Laboratories
Attn: Technical Documents Center
Fort Belvoir, Virginia 22060

ODDR&E Advisory Group on Electron Devices — 3 copies
201 Varick Street
New York, New York 10014

New York Area Office — 1 copy
Office of Naval Research
715 Broadway, 5th Floor
New York, New York 10003

Air Force Weapons Laboratory — 1 copy
Technical Library
Kirtland Air Force Base
Albuquerque, New Mexico 87117

Air Force Avionics Laboratory — 1 copy
Air Force Systems Command
Technical Library
Wright-Patterson Air Force Base
Dayton, Ohio 45433

Lawrence Livermore Laboratory — 1 copy
Attn: Dr. W. F. Krupke
University of California
P. O. Box 808
Livermore, California 94550

Harry Diamond Laboratories — 1 copy
Technical Library
Connecticut Ave. at Van Ness, N. W.
Washington, D. C. 20008

Naval Air Development Center — 1 copy
Attn: Technical Library
Johnsville
Warminster, Pennsylvania 18974

Naval Weapons Center — 1 copy
Technical Library (Code 753)
China Lake, California 93555

Naval Training Equipment Center — 1 copy
Technical Library
Orlando, Florida 32813

Naval Underwater Systems Center — 1 copy
Technical Library
New London, Connecticut 06320

Commandant of the Marine Corps — 1 copy
Scientific Advisor (Code RD-1)
Washington, D. C. 20380

Naval Ordnance Station — 1 copy
Technical Library
Indian Head, Maryland 20640

Naval Postgraduate School — 1 copy
Technical Library (Code 0212)
Monterey, California 93940

Naval Missile Center — 1 copy
Technical Library (Code 5632.2)
Point Mugu, California 93010

Naval Ordnance Station — 1 copy
Technical Library
Louisville, Kentucky 40214

| | |
|---|---|
| Commanding Officer<br>Ocean Research & Development Activity<br>National Space Technology Laboratories<br>Bay St. Louis, Mississippi 39520 | 1 copy |
| Naval Explosive Ordnance Disposal Facility<br>Technical Library<br>Indian Head, Maryland 20640 | 1 copy |
| Naval Electronics Laboratory Center<br>Technical Library<br>San Diego, California 92152 | 1 copy |
| Naval Undersea Center<br>Technical Library<br>San Diego, California 92132 | 1 copy |
| Naval Surface Weapons Center<br>Technical Library<br>Dahlgren, Virginia 22448 | 1 copy |
| Naval Ship Research and Development Center<br>Central Library (Code L42 and L43)<br>Bethesda, Maryland 20084 | 1 copy |
| Naval Surface Weapons Center<br>Technical Library<br>Silver Spring, Maryland 20910 | 1 copy |
| Naval Avionics Facility<br>Technical Library<br>Indianapolis, Indiana 46218 | 1 copy |